ACS Sustainable Chemistry & Engineering

Research Article

pubs.acs.org/journal/ascecg

# Exploring the Application of Sustainable Poly(propylene carbonate) Copolymer in Toughening Epoxy Thermosets

Shusheng Chen, Bin Chen, Jiashu Fan, and Jiachun Feng*

State Key Laboratory of Molecular Engineering of Polymers, Collaborative Innovation Center of Polymers and Polymer Composite Materials, Department of Macromolecular Science, Fudan University, Shanghai 200433, China

Supporting Information

**ABSTRACT:** Herein, poly(propylene carbonate) (PPC) was used as initiator for ε-caprolactone polymerization to produce the poly(ε-caprolactone)-*block*-poly(propylene carbonate)-*block*-poly(ε-caprolactone) (PCL-PPC-PCL) triblock copolymer, enabling innovative application of PPC as a toughening agent of epoxy thermosets. The interfacial interaction between PPC modifiers and epoxy was enhanced significantly because PCL blocks were miscible with epoxy matrix. The size of separated PPC modifiers decreased dramatically as the amphiphilic block copolymer formed nanophases in epoxy host. Consequently, with the incorporation of 30 wt % PCL-PPC-PCL modifier into the thermoset, the tensile elongation and the area under the stress−strain curves increased by more than 320% and 180%, respectively, compared with neat epoxy, indicating that an excellent toughening effect was achieved using this strategy. Considering that PPC possessed an ocean of attractive properties but suffered from its low glass transition temperature in implementation as mass products, this work may open up opportunities to extend the applications of PPC.

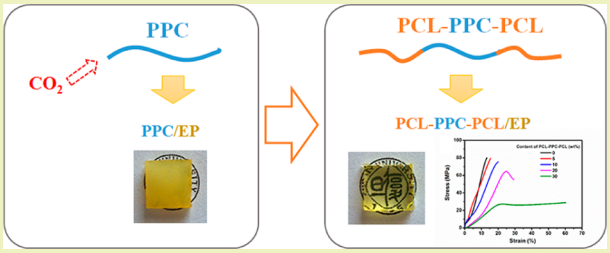


**KEYWORDS:** *Poly(propylene carbonate), Block copolymer, Epoxy, Interfacial interaction, Toughening*

## INTRODUCTION

In the past decades, a multitude of synthetic polymers, majority of which originate from nonrenewable fossil fuels, have been rapidly applied in many fields.[1] However, the application of the synthetic polymers not only consumes numerous petroleum resources but also causes serious "white pollution". With growing concerns about the energy crisis and environmental pollution, great efforts are made to develop biodegradable polymers from renewable sources.[2−4] Poly(propylene carbonate) (PPC), which is synthesized via the copolymerization of carbon dioxide and propylene oxide, has attracted increasing interest in recent years due to its high value-added fixation of $CO_2$ and its good biocompatibility and biodegradability.[5−9] Unfortunately, PPC is an amorphous polymer with low glass transition temperature ($T_g$), about 35 °C for high molecular weight (>$10^4$ g/mol) and −60 °C for low molecular weights ($10^3$ g/mol).[10] Even though PPC has been applied as specialty polymers,[11−13] its utility as mass products is still restricted by its low $T_g$. Therefore, exploring new applications of this ideal green polymer is of great importance and remains a hot issue for both academy and industry.

Epoxy thermosets are widely used as structural materials and adhesives in various industries, such as aerospace, automotive, and electronics, for their reliable mechanical properties, high heat, and solvent resistance. The distinguishing properties originate from the cross-linking chemical structure. However, owing to its high cross-linking density, epoxy thermosets are inherently of low fracture toughness, which restricts their applications.[14] During the past decades, a considerable amount of work has been made to toughen the epoxy thermosets. These studies have demonstrated that the incorporation of a second phase such as rubber particles, thermoplastic particles, or mineral fillers can improve the toughness of epoxy composites.[15−18] Considering the relative low $T_g$ of PPC, it may be used as a toughening agent for epoxy thermosets. However, to the best of our knowledge, this is only one report on toughening epoxy with PPC, in which only a little toughening effect was achieved by adding PPC.[19] The absence of favorable interfacial interaction and the size of PPC in the matrix may be responsible for the poor toughening effect. Generally, the toughening mechanisms are inclusive of debonding at the interface between the phases, limited matrix shear yielding, crack tip blunting, crack bridging, and cavitation.[20−22] The interfacial interaction between matrix and modifiers is considered as one key factor for these mechanisms to achieve excellent fracture toughness. Well-bonded modifiers locally blunt the crack tip and result in additional line tension in the crack front bowing between inclusions. Accordingly, more energy is required to propagate the crack past modifiers.[23−26] The size of the separated modifiers also plays an important role in the toughening effect.[27] For a given volume fraction of modifiers, the smaller the inclusions are, the higher the

Received: April 21, 2015
Revised: June 27, 2015
Published: July 23, 2015





DOI: 10.1021/acssuschemeng.5b00343
ACS Sustainable Chem. Eng. 2015, 3, 2077−2083

toughness achieved in the composites, which can be ascribed to increasing interfacial area between the matrix and the modifiers.[28] Moreover, experiments have shown that compared with micromodifiers, nanomodifiers confer enormous advantages to polymer composites, such as maintaining the transparency of the neat materials.[15,29] Consequently, enhancing the interfacial bonding and decreasing the size of PPC fillers in epoxy thermosets maybe one of the approaches to obtaining improved fracture toughness.

In the present work, we demonstrated the potential of modified PPC to be developed as an effective toughening agent of epoxy thermosets. Poly(ε-caprolactone)-*block*-poly(propylene carbonate)-*block*-poly(ε-caprolactone) triblock copolymer (PCL-PPC-PCL) was synthesized with PPC as the initiator. The interfacial interaction between epoxy and PPC modifier was enhanced significantly because of the well miscibility of PCL with epoxy host. Furthermore, amphiphilic block copolymers can form nanophases in epoxy matrix, which dramatically decreased the size of inclusions, and thus, fracture toughness of materials was greatly improved. Our work is the first time for functionalizing PPC with PCL for an excellent toughening agent of epoxy, extending the applications of PPC that are of great interest to the academic and industrial fields.

## EXPERIMENTAL DETAILS

**Materials.** E51 epoxy resin (EP), whose epoxide value and viscosity are 0.48−0.54 eq/100 g and 2500 mPa s (40 °C), was purchased from Bluestar Wuxi Petrochemical Co., Ltd. (Jiangsu, China). Poly(propylene carbonate) (PPC) with molecular weight of 3000 g/mol, which is terminated with hydroxyl groups, was supplied by Dazhi Environmental Protection Technology Corp. (Guangdong, China). Poly(ε-caprolactone) (PCL) was purchased from Aldrich Corp, and it had a molecular weight of 10000 g/mol. 4,4′-Methylenebis (2-chloroaniline) (MOCA), ε-caprolactone (ε-CL), stannous octanoate [$Sn(Oct)_2$], and solvents were purchased from Aladdin Reagent Corp. (Shanghai, China). The monomer of ε-CL and solvent was dried over calcium hydride ($CaH_2$) and distilled under decreased pressure prior to use. The chemical structures of epoxy, MOCA, and PPC are shown in Scheme 1.

**Synthesis of PCL-PPC-PCL Triblock Copolymer.** Poly(ε-caprolactone)-*block*-poly(propylene carbonate)-*block*-poly(ε-caprolactone) triblock copolymer (PCL-PPC-PCL) was synthesized via the ring-opening polymerization (ROP) of ε-CL in the presence of PPC with $Sn(Oct)_2$ as the catalyst.[30] Typically, 1 g (0.67 mmol with respect to hydroxyl groups of PPC) of PPC and 3 g (26.3 mmol) of ε-CL were dissolved in anhydrous toluene in a 50 mL predried Schlenk flask equipped with a magnetic stirrer, followed by the addition of 0.02 g of $Sn(Oct)_2$. After three pump freeze−thaw cycles, the flask was immersed into an oil bath, and polymerization was carried out at 120 °C for 48 h. The crude product was dissolved in a spot of tetrahydrofuran (THF), and the solution was dropped into a great amount of petroleum ether to afford the precipitates. The collected production was dried in a vacuum oven at 40 °C for 24 h.

**Scheme 1. Chemical Structures of (a) Epoxy, (b) MOCA, and (c) PPC**

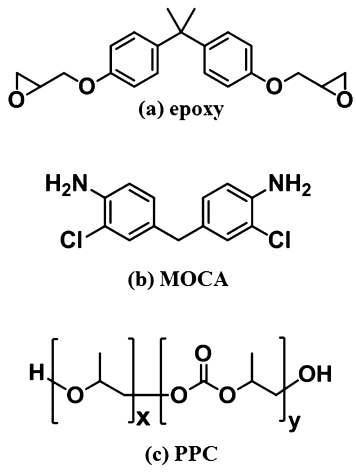


**Preparation of PCL-PPC-PCL/EP Thermosets.** The desired amount of the PCL-PPC-PCL triblock copolymer was added to EP with continuous stirring at 100 °C until the mixtures became homogeneous and transparent. The curing agent MOCA was added with stirring until full dissolution. The mixtures were poured into preheated polytetrafluoroethylene molds and then cured at 150 °C for 2.5 h and post-cured at 180 °C for 2.5 h. Following a similar procedure, neat EP, PPC/EP, and PPC-PCL-PPC specimens were prepared as references.

**Characterization.** Fourier transform infrared (FTIR) spectra were recorded using a Nicolet spectrometer. Nuclear magnetic resonance (NMR) spectra of the samples were recorded by a Varian Mercury plus 400 spectrometer with deuterated chloroform as solvent and tetramethylsilane as the internal reference. A gel permeation chromatography (GPC) instrument with a G1362A refractive index detector was used to determine the weight-average molecular weights ($M_w$), number-average molecular weights ($M_n$), and polydispersity index (PDI, $M_w/M_n$). THF was employed as the eluent at a flow rate of 1.0 mL/min, and the calibration curve was obtained with monodispersed polystyrene as the standards.

The fractured surfaces of the EP blends were obtained under cryogenic condition using liquid nitrogen, followed by etching in THF at room temperature for 12 h. The morphologies of etched surfaces were observed by a Zeiss Ultra 55 field-emission scanning electron microscopy (SEM) at an operating voltage of 5 kV. The morphological observation of the samples was conducted on a Multimode 8 atomic force microscope (AFM) in the tapping mode. The specimens for AFM observation were prepared using an ultramicrotome (Leica FC7-UC7) equipped with a diamond knife. Dynamic mechanical analysis (DMA, Mettler-Toledo DMA/SDTA861e) was conducted to measure the glass transition temperature ($T_g$) of composites. The specimen dimensions for DMA measurement were 30 mm × 4.0 mm × 2.0 mm. The testing was performed in dual cantilever mode at multi-frequencies of 1 Hz with a heating rate of 5 °C/min between −100 and 200 °C. Mechanical properties were measured at 23 °C and ∼40% relative humidity using a SANS CMT-4102 universal testing machine (Shenzhen, China) at a crosshead speed of 1 mm/min. The specimens have a dimension of 50 mm (length) × 8.0 mm (width) × 20 mm (narrow portion length) × 4.0 mm (narrow portion width) × 2.0 mm (thickness). At least five tests were performed for each sample, from which mean values and standard deviations were derived. Differential scanning calorimetry (DSC, TA Q2000) was used to investigate the $T_g$ of PPC at a heating rate of 10 °C/min from −80 to 10 °C under nitrogen atmosphere.

## RESULTS AND DISCUSSION

**Characterization of Triblock Copolymer.** The routes of syntheses for the PCL-PPC-PCL triblock copolymers are shown in Scheme 2. The ROPs of ε-CL were carried out with PPC as the macromolecular initiators and $Sn(Oct)_2$ as the catalyst. This polymerization was carried out at 120 °C for 48 h to obtain a complete conversion of the monomer.

The FTIR spectra of PPC, PCL, and PCL-PPC-PCL are shown in Figure 1. The characteristic absorption bands for PPC are attributed to the stretching vibration of C−H at 2800−2900 $cm^{-1}$, C═O at 1750 $cm^{-1}$, and C−O−C band at 1100 $cm^{-1}$. Particularly, the absorption peaks at 2980 and 2901 $cm^{-1}$ and 2937 and 2877 $cm^{-1}$ correspond to the stretching vibrations of $-CH_3$ and $-CH_2$ in PPC, respectively. As to PCL-PPC-PCL,


DOI: 10.1021/acssuschemeng.5b00343
ACS Sustainable Chem. Eng. 2015, 3, 2077−2083

**Scheme 2. Synthesis of PCL-PPC-PCL Triblock Copolymer**

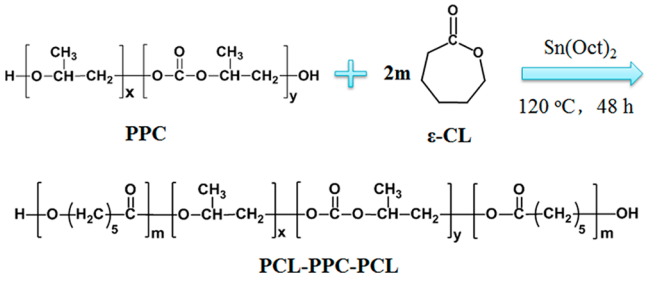


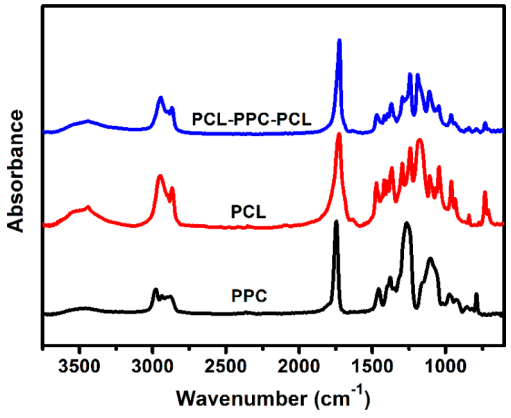


**Figure 1.** FTIR spectra of PPC, PCL, and PCL-PPC-PCL.

the intensity of bands corresponding to the $-CH_2$ stretching vibration is remarkably increased due to only the content of $-CH_2$ in the PCL blocks. The peak associated with the C═O stretching vibration of PCL-PPC-PCL shifts to 1725 $cm^{-1}$, which is induced by the shearing vibration of C═O group in the PCL subchains. The results of FTIR indicate that the PCL-PPC-PCL triblock copolymer is successfully obtained.

Figure 2 shows the $^1$H NMR spectrum of the PCL-PPC-PCL triblock copolymer. The signals of resonance at 1.3−1.5 ppm are assignable to the methyl groups of PPC subchains. The characteristic peaks of methylene and methine groups in the PPC subchains are assigned as follows: $^1$H NMR ($CDCl_3$), $\delta$ (ppm) 3.2−3.7 (2H, 1H; $-CH_2CHOCH_2CHO-$), 4.0−4.3

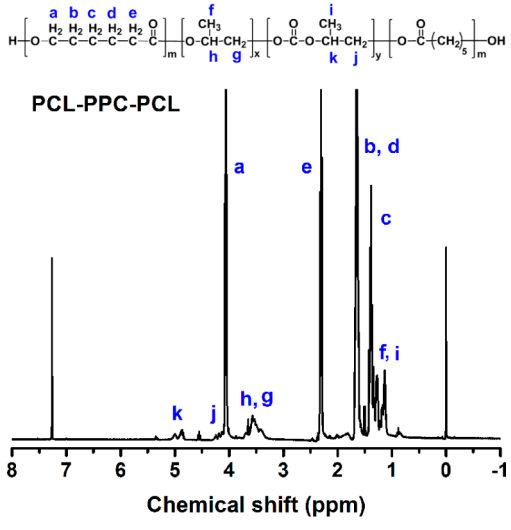


**Figure 2.** $^1$H NMR spectrum of PCL-PPC-PCL triblock copolymer.

(2H; $-OCOCH_2CH-$), 4.7−5.0 (1H; $-OCOCH_2CH-$), which can be found in the $^1$H NMR spectrum of pure PPC (Figure S1a). As to PCL-PPC-PCL, the additional signals of resonance from the PCL blocks are detected at 1.4, 1.7, 2.3, and 4.1 ppm, which are assignable to the protons of methylene of PCL subchains (Figure S1b). As indicated in the $^1$H NMR spectrum, the simultaneous appearance of the resonance characteristic of PPC and PCL protons implies that the resulting product combines the structural features of PPC and PCL, which means that the PCL-PPC-PCL triblock copolymer is successfully obtained.

The molecular weights and corresponding polydispersity indices (PDI) of PPC and PCL-PPC-PCL were determined by GPC, and their GPC curves are shown in Figure 3. The GPC

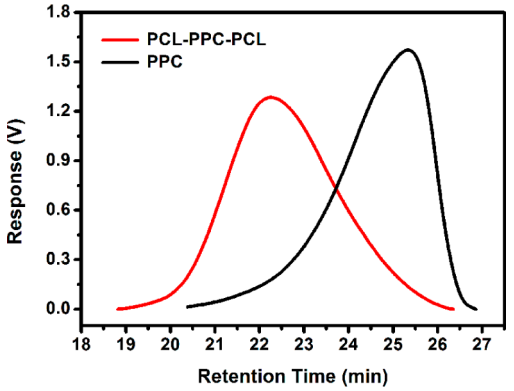


**Figure 3.** GPC curves of PPC and PCL-PPC-PCL triblock copolymer.

trace of PCL-PPC-PCL displays a unimodal peak, confirming that the triblock copolymer is successfully prepared. The molecular weight of PCL-PPC-PCL is estimated to be $M_n$ = 11,400 g/mol, and thereby the lengths of PCL blocks in the triblock copolymer are calculated to $L_{PCL}$ = 4200 g/mol.

**Characterization of the PCL-PPC-PCL/EP Thermosets.** Before curing, all the systems of epoxy precursors, curing agents, and PCL-PPC-PCL (or PPC) were homogeneous and transparent at room and elevated temperatures. This observation is consistent with the previous report that PPC is miscible with EP precursors and reaction-induced phase separation occurs during the curing.[31] Figure 4 shows the photographs of neat EP and thermosetting blends. After curing at a setting temperature, the thermosetting blend containing PPC and PCL homopolymers becomes cloudy, implying the occurrence of macroscopic phase separation. However, all the thermosets containing the PCL-PPC-PCL triblock copolymer are transparent and homogeneous, which suggests that no macroscopic phase separation occurred at least on the scale exceeding the wavelength of visible light.

The SEM micrograph of THF-etched fracture surfaces of the thermoset containing 3 wt % PPC and 7 wt % PCL is shown in Figure 5. It is shown that the spherical pores are uniformly dispersed in the continuous EP matrix after PPC phases are rinsed by THF. The diameter of spherical phases is about 1 $\mu$m, which confirms occurrence of macroscopic phase separation in the PPC/PCL/EP system. However, for the thermoset containing 10 wt % PCL-PPC-PCL triblock copolymer, no pore can be observed under the same magnification after an identical etched condition (Figure S2), thus demonstrating the absence of macroscopic phase separation in the PCL-PPC-PCL/EP blends.


DOI: 10.1021/acssuschemeng.5b00343
ACS Sustainable Chem. Eng. 2015, 3, 2077−2083

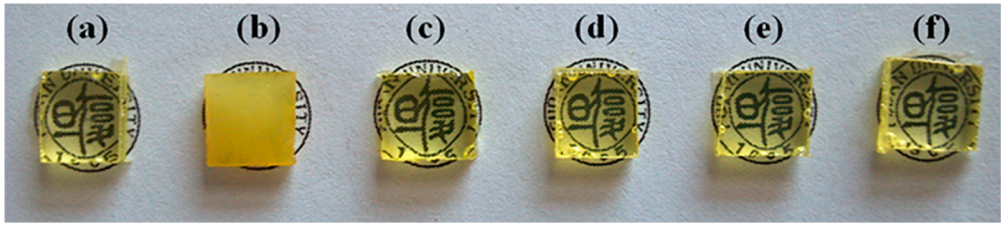


**Figure 4.** Photographs of (a) neat EP, (b) PPC/PCL/EP (3/7/90) blend, and thermosets containing (c) 5, (d) 10, (e) 20, and (f) 30 wt % of PCL-PPC-PCL.

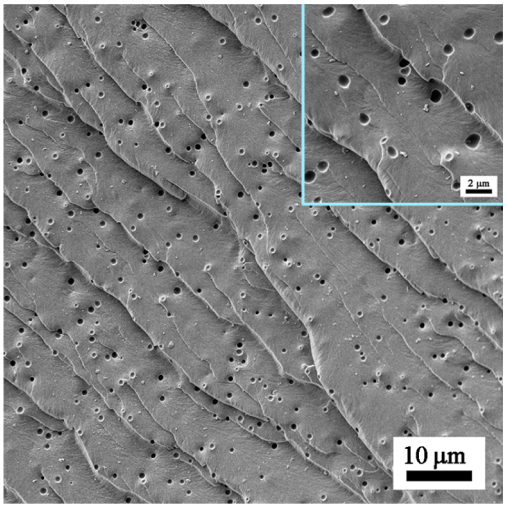


**Figure 5.** SEM micrograph of THF-etched fracture surfaces of PPC/PCL/EP (3/7/90) blend. Insert is image at different magnification.

Atomic force microscopy (AFM) was carried out to observe the morphology of EP thermosets containing the PCL-PPC-PCL triblock copolymer after reaction-induced phase separation. As shown in Figure 6, the upper part of each micrograph is the topography image and the lower part is the phase image. The topography images show that the surfaces of the as-prepared specimens are quite smooth and free of visible defects. In terms of the difference in viscoelastic properties between EP and PPC phases, the light continuous regions are ascribed to the EP matrix, while the dark regions are attributed to PPC domains. It is deducible from the SEM and AFM results of the PPC/PCL/EP blend that dark regions are corresponding to the PPC domains etched by THF (Figure 5 and Figure S3). It is obvious that all the blends containing the PCL-PPC-PCL triblock copolymer exhibit nanostructured morphology, which is in accordance with the previous studies that PCL is miscible with several amine-cured epoxy systems[32−34] and amphiphilic block copolymers can form nanophases in epoxy matrix.[35−41] The long worm-like PPC micelles with an average size in diameter of 5−20 nm are uniformly dispersed into the continuous EP matrix. The sizes of the dispersed PPC nanophases increase with increasing the content of PCL-PPC-PCL in the EP thermosets. The results of AFM observation verify that microphase separation occurs during the curing for the thermosets containing PCL-PPC-PCL triblock copolymer and the sizes of separated PPC phases decrease into nanoscale compared with PPC/PCL/EP system.

To ascertain the miscibility of the cross-linked EP networks with PCL and PPC blocks, a DMA technique was employed. As shown in Figure 7a, the neat EP exhibited a well-defined $T_g$ ($\alpha$ transition) at 146 °C. Apart from $\alpha$ transition, it exhibits a secondary relaxation peak ($\beta$ transition) from about −50 to −60 °C. This transition is predominantly attributed to the motion of hydroxyl ether structural units and diphenyl groups in epoxy.[42] Since the $T_g$ of PPC is about −53 °C (Figure S4), the $\alpha$ transition of PPC nanodomains is overlapped with the $\beta$ transition of epoxy in PCL-PPC-PCL/EP thermosets. Therefore, it is difficult to distinguish $T_g$ of PPC in the Tan $\delta$ vs temperature curves of thermosets containing the PCL-PPC-PCL triblock copolymer. Upon adding the PCL-PPC-PCL triblock copolymer into the thermosets, the $T_g$ of the matrix shifts to a lower temperature. The $T_g$ of the EP matrix decreases with increasing the content of the PCL-PPC-PCL triblock copolymer, which indicates the miscibility of the PCL subchains and EP matrix.

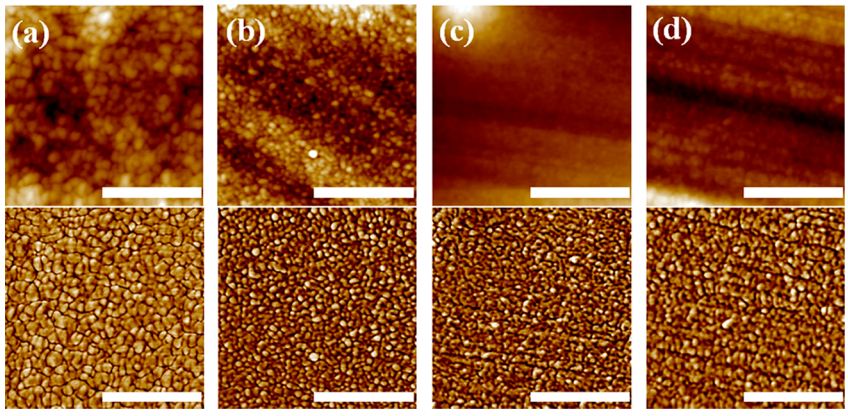


**Figure 6.** AFM images of the EP thermosets containing (a) 5, (b) 10, (c) 20, and (d) 30 wt % of PCL-PPC-PCL triblock copolymer. Top: topography. Bottom: phase contrast images. White bar indicates 500 nm in all images.


DOI: 10.1021/acssuschemeng.5b00343
ACS Sustainable Chem. Eng. 2015, 3, 2077−2083

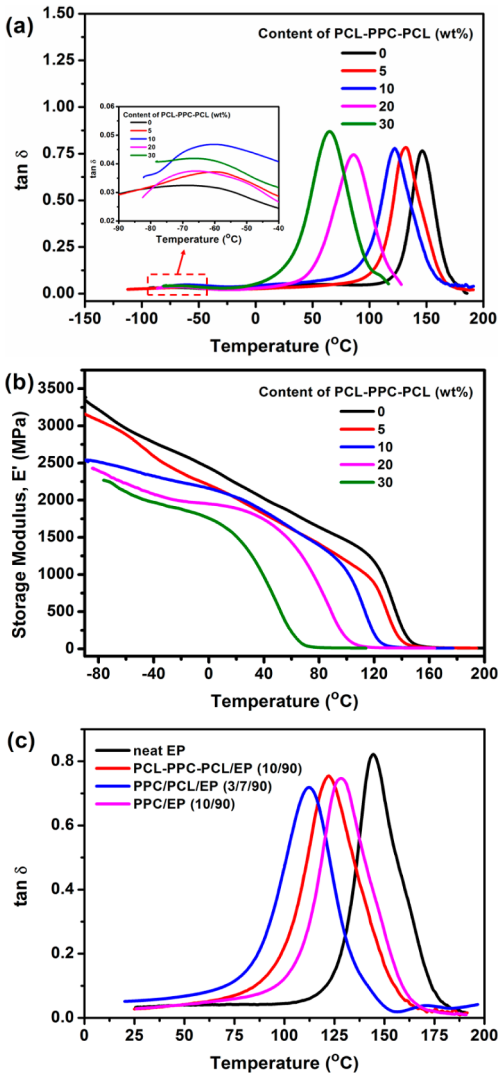


**Figure 7.** (a) Tan $\delta$ vs temperature curves and (b) storage modulus ($E'$) of neat EP and thermosets containing PCL-PPC-PCL triblock copolymer, (c) Tan $\delta$ vs temperature curves of neat EP, PCL-PPC-PCL/EP (10/90), PPC/PCL/EP (3/7/90), and PPC/EP (10/90) blends.

DMA is also a powerful tool used to evaluate the density of cross-linking of thermosets. The cross-link density ($\upsilon$) of the EP networks can be calculated using the following rubber elasticity equation $\upsilon = E'/3RT$, where $R$ is the gas constant and $T$ is the absolute temperature in rubbery plateau region ($T_g$ + 30 K).[43] The storage modulus ($E'$) of the PCL-PPC-PCL/EP thermosets is presented in Figure 7b. The $\upsilon$ values calculated from $E'$ in the rubbery plateau region are given in Table 1. It is noteworthy that the cross-link densities of neat EP and PCL-PPC-PCL/EP thermosets are similar, which indicates that the addition of the PCL-PPC-PCL triblock copolymer into the thermosets does not affect the degree of curing of the EP networks. Since the $T_g$ values of EP in thermosets are influenced by plasticizers and cross-link density, the low $T_g$ of EP in PCL-PPC-PCL/EP thermoset is not likely due to low cross-link density but rather to the plasticization of PCL subchains, which promote the mobility of epoxy chains.

In order to verify this conclusion, the $T_g$ values of EP in PPC/PCL/EP (3/7/90) and PPC/EP (10/90) blends were also determined. Figure 7c shows that the EP in PPC/EP (10/90) blend displays higher $T_g$ than that in the PCL-PPC-PCL/EP (10/90) blend, which originates from the well miscibility of PCL subchains with the EP host. Hence, the interfacial interaction between the matrix and modifier in the PCL-PPC-PCL/EP thermoset is significantly stronger than that in the PPC/EP blend. It is interesting to note that with similar composition, the $T_g$ of EP in the PCL-PPC-PCL/EP (10/90) blend is significantly higher than that in PPC/PCL/EP (3/7/90) blend. As suggested by previous reports,[44] a possible explanation for the difference is that the PCL subchains have to be enriched at the surface of the microphase-separated PPC nanodomains in the nanostructured PCL-PPC-PCL/EP thermosets due to chemical bonds between PPC and PCL blocks. However, PCL homopolymer is homogeneously dispersed into the EP matrix, and thereby, the EP matrix is well plasticized. Therefore, the $T_g$ results indicate that the addition of the PCL-PPC-PCL modifier into the EP matrix not only generates an superior interfacial bonding but also maintains the relatively satisfying thermal property of the matrix.

The toughening effect of PCL-PPC-PCL on the thermosets was evaluated by tensile testing, whose results and representative curves are given in Figure 8. In spite of the decrease in tensile strength, it is evident that the incorporation of the PCL-PPC-PCL modifier sharply increases the elongation at break of the resulting thermosets. The toughness of the PCL-PPC-PCL/EP thermosets, which relates to overall energy dissipation, is obtained by calculating the area under the stress−strain curves. The elongation and toughness of neat EP present the values of 13 ± 1% and 4.7 ± 0.5 MJ/m$^3$, respectively. With the incorporation of 5, 10, 20, and 30 wt % of PCL-PPC-PCL modifiers, the elongation values of the PCL-PPC-PCL/EP thermosets increase by 15%, 48%, 107%, and 323%, respectively, while the toughness values increased for 35%, 58%, 98%, and 182%, respectively. According to a previous study, the improvement in fracture toughness of worm-like nanostructured thermosets is likely to derive from a combination of several toughening mechanisms: voiding or debonding at the interface between the phases, limited matrix shear yielding, crack tip blunting, crack bridging, and viscoelastic energy dissipation.[45] It is worth mentioning that a favorable interface plays an important role on these mechanisms for energy dissipation. Compared with the

**Table 1. $T_g$, Storage Modulus ($E'$) at $T_g$ + 30 K and Cross-Link Density ($\upsilon$) of Neat EP and Thermosets Containing PCL-PPC-PCL Triblock Copolymer**

| | content of PCL-PPC-PCL | | | | |
|---|---|---|---|---|---|
| | 0 wt % | 5 wt % | 10 wt % | 20 wt % | 30 wt % |
| $T_g$ (K) | 419 | 404 | 395 | 365 | 338 |
| $E'$ at $T_g$ + 30 K (MPa) | 12.6 | 14.3 | 9.7 | 10.0 | 11.22 |
| $\upsilon$ ( × 10$^3$ mol m$^{-3}$) | 1.12 | 1.32 | 0.92 | 1.02 | 1.22 |


DOI: 10.1021/acssuschemeng.5b00343
ACS Sustainable Chem. Eng. 2015, 3, 2077−2083

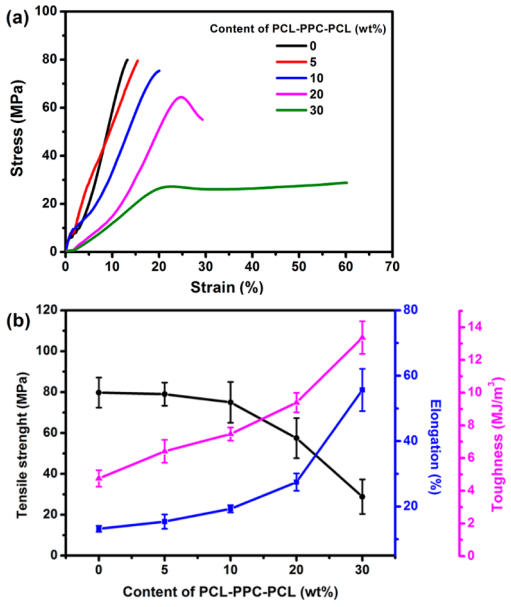


**Figure 8.** (a) Representative tensile curves, (b) tensile strength, elongation, and toughness of neat EP and thermosets containing PCL-PPC-PCL triblock copolymer.

thermosets modified with PPC at the micrometer scale, the excellent toughness improvement of the thermosets via the formation of the nanostructures may be caused by two reasons. The first and foremost, the interfacial interaction between the matrix and PPC nanophases is significantly enhanced due to the miscibility of the PCL blocks with the EP thermosets. Second, the PPC toughening phase is homogeneously dispersed in the EP matrix at the nanometer scale, which will greatly increase the interfacial area between the matrix and the modifier. As a result, the PCL-PPC-PCL modifier possesses an excellent toughening effect for EP thermosets in spite of sacrificing part of the strength and thermal property of the matrix. The approaches to avoid this disadvantage will be the subject of future investigations.

## CONCLUSION

In summary, we have explored an innovative application of PPC as an effective toughening agent of EP thermosets. PCL-PPC-PCL triblock copolymer was synthesized successfully with PPC as the initiator, which was testified by FTIR, $^1$H NMR, and GPC characterizations. The interfacial interaction and size of separated PPC blocks are optimized significantly, which is confirmed by SEM, AFM, and DMA characterizations. As a consequence, excellent toughness of PCL-PPC-PCL modified thermosets is achieved in spite of sacrificing part of the strength and thermal properties of the matrix. Therefore, this work broadens the applications of PPC and promotes its implementation as mass products.

## ASSOCIATED CONTENT

### Supporting Information

The Supporting Information is available free of charge on the ACS Publications website at DOI: 10.1021/acssuschemeng.5b00343.

$^1$H NMR spectra of PPC and PCL homopolymers. SEM micrograph of THF-etched fracture surfaces of PCL-PPC-PCL/EP (10/90). AFM images of PPC/PCL/EP (3/7/90) blend. DSC curve of PPC homopolymer. (PDF)

## AUTHOR INFORMATION

### Corresponding Author

*E-mail: jcfeng@fudan.edu.cn. Tel: 86 (21) 6564 3735. Fax: +86- 21-6564 0293.

### Notes

The authors declare no competing financial interest.

## ACKNOWLEDGMENTS

This work was financially supported by the Natural Science Foundation of China (21174032) and National Basic Research Program of China (2011CB605704).

## REFERENCES

(1) Ray, S. S.; Bousmina, M. Biodegradable polymers and their layered silicate nanocomposites: In greening the 21st century materials world. *Prog. Mater. Sci.* **2005**, *50*, 962−1079.
(2) Gross, R. A.; Kalra, B. Biodegradable polymers for the environment. *Science* **2002**, *297*, 803−807.
(3) Okada, M. Chemical syntheses of biodegradable polymers. *Prog. Polym. Sci.* **2002**, *27*, 87−133.
(4) Wang, D.; Yu, J.; Zhang, J.; He, J.; Zhang, J. Transparent bionanocomposites with improved properties from poly(propylene carbonate) (PPC) and cellulose nanowhiskers (CNWs). *Compos. Sci. Technol.* **2013**, *85*, 83−89.
(5) Inoue, S.; Koinuma, H.; Tsuruta, T. Copolymerization of carbon dioxide and epoxide. *J. Polym. Sci., Part B: Polym. Lett.* **1969**, *7*, 287−292.
(6) Luinstra, G. A. Poly(propylene carbonate), old copolymers of propylene oxide and carbon dioxide with new interests: Catalysis and material properties. *Polym. Rev.* **2008**, *48*, 192−219.
(7) Yang, G.; Geng, C.; Su, J.; Yao, W.; Zhang, Q.; Fu, Q. Property reinforcement of poly(propylene carbonate) by simultaneous incorporation of poly(lactic acid) and multiwalled carbon nanotubes. *Compos. Sci. Technol.* **2013**, *87*, 196−203.
(8) Hu, X.; Xu, C.; Gao, J.; Yang, G.; Geng, C.; Chen, F.; Fu, Q. Toward environment-friendly composites of poly(propylene carbonate) reinforced with cellulose nanocrystals. *Compos. Sci. Technol.* **2013**, *78*, 63−68.
(9) Li, Y.; Shimizu, H. Compatibilization by homopolymer: Significant improvements in the modulus and tensile strength of PPC/PMMA blends by the addition of a small amount of PVAc. *ACS Appl. Mater. Interfaces* **2009**, *1*, 1650−1655.
(10) Liu, B.; Chen, L.; Zhang, M.; Yu, A. Degradation and stabilization of poly(propylene carbonate). *Macromol. Rapid Commun.* **2002**, *23*, 881−884.
(11) Welle, A.; Kröger, M.; Döring, M.; Niederer, K.; Pindel, E.; Chronakis, I. S. Electrospun aliphatic polycarbonates as tailored tissue scaffold materials. *Biomaterials* **2007**, *28*, 2211−2219.
(12) Wang, D.; Kang, M.; Wang, X. Aliphatic Polycarbonates Synthesized with Carbon Dioxide. *Prog. Chem.* **2002**, *14*, 462−468.
(13) Lu, Q.; Gao, Y.; Zhao, Q.; Li, J.; Wang, X.; Wang, F. Novel polymer electrolyte from poly(carbonate-ether) and lithium tetrafluoroborate for lithium-oxygen battery. *J. Power Sources* **2013**, *242*, 677−682.
(14) May, C. A. In *Epoxy Resins: Chemistry and Technology*, 2nd ed.; May, C. A., Ed.; Dekker: New York, 1988.
(15) Jordan, J.; Jacob, K. I.; Tannenbaum, R.; Sharaf, M. A.; Jasiuk, I. Experimental trends in polymer nanocomposites - A review. *Mater. Sci. Eng., A* **2005**, *393*, 1−11.
(16) Johnsen, B. B.; Kinloch, A. J.; Mohammed, R. D.; Taylor, A. C.; Sprenger, S. Toughening mechanisms of nanoparticle-modified epoxy polymers. *Polymer* **2007**, *48*, 530−541.


DOI: 10.1021/acssuschemeng.5b00343
*ACS Sustainable Chem. Eng.* 2015, 3, 2077−2083

(17) Liu, W.; Zhou, R.; Goh, H. L. S.; Huang, S.; Lu, X. From waste to functional additive: Toughening epoxy resin with lignin. *ACS Appl. Mater. Interfaces* **2014**, *6*, 5810−5817.
(18) González-Domínguez, J. M.; Ansón-Casaos, A.; Díez-Pascual, A. M.; Ashrafi, B.; Naffakh, M.; Backman, D.; Stadler, H.; Johnston, A.; Gómez, M.; Martínez, M. T. Solvent-free preparation of high-toughness epoxy-SWNT composite materials. *ACS Appl. Mater. Interfaces* **2011**, *3*, 1441−1450.
(19) Huang, Y.; Wang, J.; Liao, B.; Chen, M.; Cong, G. Epoxy resins toughened by poly(propylene carbonate). *J. Appl. Polym. Sci.* **1997**, *64*, 2457−2465.
(20) Pearson, R. A.; Yee, A. F. Toughening mechanisms in elastomer-modified epoxies - Part 2 Microscopy studies. *J. Mater. Sci.* **1986**, *21*, 2475−2488.
(21) Yee, A. F.; Pearson, R. A. Toughening mechanisms in elastomer-modified epoxies - Part 1 Mechanical studies. *J. Mater. Sci.* **1986**, *21*, 2462−2474.
(22) Pearson, R. A.; Yee, A. F. Toughening mechanisms in elastomer-modified epoxies - Part 3 The effect of cross-link density. *J. Mater. Sci.* **1989**, *24*, 2571−2580.
(23) Odegard, G. M.; Clancy, T. C.; Gates, T. S. Modeling of the mechanical properties of nanoparticle/polymer composites. *Polymer* **2005**, *46*, 553−562.
(24) Chen, L.; Chai, S.; Liu, K.; Ning, N.; Gao, J.; Liu, Q.; Chen, F.; Fu, Q. Enhanced epoxy/silica composites mechanical properties by introducing graphene oxide to the interface. *ACS Appl. Mater. Interfaces* **2012**, *4*, 4398−4404.
(25) Khare, K. S.; Khabaz, F.; Khare, R. Effect of carbon nanotube functionalization on mechanical and thermal properties of cross-linked epoxy-carbon nanotube nanocomposites: Role of strengthening the interfacial interactions. *ACS Appl. Mater. Interfaces* **2014**, *6*, 6098−6110.
(26) Martinez-Rubi, Y.; Ashrafi, B.; Guan, J.; Kingston, C.; Johnston, A.; Simard, B.; Mirjalili, V.; Hubert, P.; Deng, L.; Young, R. J. Toughening of epoxy matrices with reduced single-walled carbon nanotubes. *ACS Appl. Mater. Interfaces* **2011**, *3*, 2309−2317.
(27) Liang, Y. L.; Pearson, R. A. Toughening mechanisms in epoxy-silica nanocomposites (ESNs). *Polymer* **2009**, *50*, 4895−4905.
(28) Bagheri, R.; Pearson, R. A. Role of particle cavitation in rubber-toughened epoxies: 1. Microvoid toughening. *Polymer* **1996**, *37*, 4529−4538.
(29) De, B.; Voit, B.; Karak, N. Transparent luminescent hyperbranched epoxy/carbon oxide dot nanocomposites with outstanding toughness and ductility. *ACS Appl. Mater. Interfaces* **2013**, *5*, 10027−10034.
(30) Meng, F.; Zheng, S.; Zhang, W.; Li, H.; Liang, Q. Nanostructured thermosetting blends of epoxy resin and amphiphilic poly(ε-caprolactone)-block-polybutadiene-block-poly(ε-caprolactoné) triblock copolymer. *Macromolecules* **2006**, *39*, 711−719.
(31) Li, J.; Du, Z.; Li, H.; Zhang, C. Chemically induced phase separation in the preparation of porous epoxy monolith. *J. Polym. Sci., Part B: Polym. Phys.* **2010**, *48*, 2140−2147.
(32) Chen, J. L.; Huang, H. M.; Li, M. S.; Chang, F. C. Transesterification in homogeneous poly(ε-caprolactone)-epoxy blends. *J. Appl. Polym. Sci.* **1999**, *71*, 75−82.
(33) Guo, Q.; Groeninckx, G. Crystallization kinetics of poly(ε-caprolactone) in miscible thermosetting polymer blends of epoxy resin and poly(ε-caprolactone). *Polymer* **2001**, *42*, 8647−8655.
(34) Guo, Q.; Harrats, C.; Groeninckx, G.; Reynaers, H.; Koch, M. H. J. Miscibility, crystallization and real-time small-angle X-ray scattering investigation of the semicrystalline morphology in thermosetting polymer blends. *Polymer* **2001**, *42*, 6031−6041.
(35) Hillmyer, M. A.; Lipic, P. M.; Hajduk, D. A.; Almdal, K.; Bates, F. S. Self-assembly and polymerization of epoxy resin-amphiphilic block copolymer nanocomposites. *J. Am. Chem. Soc.* **1997**, *119*, 2749−2750.
(36) Lipic, P. M.; Bates, F. S.; Hillmyer, M. A. Nanonstructured thermosets from self-assembled amphiphilic block copolymer/epoxy resin mixtures. *J. Am. Chem. Soc.* **1998**, *120*, 8963−8970.
(37) Mijovic, J.; Shen, M.; Sy, J. W.; Mondragon, I. Dynamics and morphology in nanostructured thermoset network/block copolymer blends during network formation. *Macromolecules* **2000**, *33*, 5235−5244.
(38) Guo, Q.; Thomann, R.; Gronski, W.; Thurn-Albrecht, T. Phase behavior, crystallization, and hierarchical nanostructures in self-organized thermoset blends of epoxy resin and amphiphilic poly(ethylene oxide)-block-poly(propylene oxide)-block-poly(ethylene oxide) triblock copolymers. *Macromolecules* **2002**, *35*, 3133−3144.
(39) Rebizant, V.; Venet, A. S.; Tournilhac, F.; Girard-Reydet, E.; Navarro, C.; Pascault, J. P.; Leibler, L. Chemistry and mechanical properties of epoxy-based thermosets reinforced by reactive and nonreactive SBMX block copolymers. *Macromolecules* **2004**, *37*, 8017−8027.
(40) Meng, F.; Zheng, S.; Li, H.; Liang, Q.; Liu, T. Formation of ordered nanostructures in epoxy thermosets: A mechanism of reaction-induced microphase separation. *Macromolecules* **2006**, *39*, 5072−5080.
(41) Romeo, H. E.; Zucchi, I. A.; Rico, M.; Hoppe, C. E.; Williams, R. J. J. From spherical micelles to hexagonally packed cylinders: The cure cycle determines nanostructures generated in block copolymer/epoxy blends. *Macromolecules* **2013**, *46*, 4854−4861.
(42) Xu, Z.; Zheng, S. Reaction-induced microphase separation in epoxy thermosets containing poly(ε-caprolactone)-block-poly(n-butyl acrylate) diblock copolymer. *Macromolecules* **2007**, *40*, 2548−2558.
(43) Hill, L. W. Calculation of crosslink density in short chain networks. *Prog. Org. Coat.* **1997**, *31*, 235−243.
(44) Yang, X.; Yi, F.; Xin, Z.; Zheng, S. Morphology and mechanical properties of nanostructured blends of epoxy resin with poly(ε-caprolactone)-block-poly(butadiene-co-acrylonitrile)-block-poly(ε-caprolactone) triblock copolymer. *Polymer* **2009**, *50*, 4089−4100.
(45) Liu, J.; Thompson, Z. J.; Sue, H. J.; Bates, F. S.; Hillmyer, M. A.; Dettloff, M.; Jacob, G.; Verghese, N.; Pham, H. Toughening of epoxies with block copolymer micelles of wormlike morphology. *Macromolecules* **2010**, *43*, 7238−7243.


DOI: 10.1021/acssuschemeng.5b00343
*ACS Sustainable Chem. Eng.* 2015, 3, 2077−2083